An empirical approach to estimating hydrocarbon column heights for improved

pre-drill volume prediction in hydrocarbon exploration

Edmundson, I.[1], Davies, R.[2], Frette, L.U.[3], Mackie, S.[2], Kavli, E.A.[4], Rotevatn, A.[1],

Yielding, G.[5], Dunbar, A.[2]

[1] Department of Earth Science, University of Bergen, Allégaten 41, 5007 Bergen,

Norway

[2] DEA Norge AS, Jåttåflaten 27, 4007 Stavanger, Norway

[3] Capricorn Energy, Jåttåvågveien 7, 4020 Stavanger, Norway

[4] IFP School, 232 Avenue Napoléon Bonaparte, 92852 Rueil-Malmaison, France

[5] Badley Geoscience Ltd, North Beck House, North Beck Lane, Hundleby, Spilsby

Lincolnshire, PE23 5NB, UK

isabel.edmundson@uib.no, roy.davies@wintershalldea.com,

lars.ulsund.frette@gmail.com, sean.mackie@wintershalldea.com,

emilieak@online.no, atle.rotevatn@uib.no, graham@badleys.co.uk,

alex.b.dunbar@gmail.com

Abstract

29   Estimating pre-drill volumes in hydrocarbon exploration involves dealing with

30   geological and technical uncertainties. The prediction of the hydrocarbon column

31   height is widely recognized as the primary driver of uncertainty in volumetric

32   estimates. The oil and gas industry continues to renew efforts to limit such

33   uncertainties because of the potential economic costs of inaccurate estimation, yet

34   estimation of pre-drill volumes remains an in-exact science. This study introduces

35   new empirical data from the Norwegian Continental Shelf, and aims to improve

36   accuracy in hydrocarbon column height prediction. We use column height, trap height

37   and burial depth data to calculate the degree of hydrocarbon trap fill for each of the

38   242 studied discovery wells. The data is aggregated into a simple forward probability

39   model to calculate the probability of encountering different ranges of trap-fill, based

40   on burial depth and trap height. The distribution of trap-fill ratios clearly correlates

41   with both trap height and burial depth, thus indicating that the same pre-drill column

42   height distribution should not be used for all prospects. These findings strongly

43   suggest that the prospect's dimensions and burial depth are used alongside other

44   technical subsurface factors to determine the most suitable pre-drill hydrocarbon

45   column height distribution. This method contributes to reducing the largest source of

46   uncertainty, which in turn reduces the overall uncertainty associated with pre-drill

47   volume estimation. Such an approach will increase the accuracy of pre-drill volume

48   estimation, leading to more appropriate future development plans. We recommend

49   that the presented methods and lessons learnt are applied in basins settings

50   worldwide.

1. Introduction

52   Estimating pre-drill volumes is an essential part of the exploration process that

53   determines if a prospect contains a large enough volume of hydrocarbons to justify

54   drilling an exploration or appraisal well. Yet, despite its importance and an overall

55   improvement in available technology, the industry continues to be poor at estimating

56   pre-drill hydrocarbon volumes (Milkov, 2017). This is largely the result of uncertainty

57   associated with each of the ten main inputs required to calculate potential

58   hydrocarbon volumes (Table 1). Combining these inputs further compounds the level

59   of uncertainty resulting in errors, which can lead to surprises and often

60   disappointment once volumes are reassessed after drilling (Garb, 1988; Skaar et al.,

61   2000; Demirmen, 2007). Of all of the inputs, the hydrocarbon column height

62   uncertainty generally has the largest impact on the calculated pre-drill volume range

63   (Fig. 1). Despite this, efforts to constrain the column height are commonly bypassed

64   in favor of work that focuses on other inputs required to calculate pre-drill volumes

65   that carry far less uncertainty. Instead, we argue that constraining the hydrocarbon

66   column distribution should be prioritized for the benefit of reducing the overall

67   uncertainty of reserve estimation (Floris and Peersmann, 1998).

68   Hydrocarbon column heights have perhaps remained as one of the key uncertainties

69   in reserve calculations because of the difficulty in obtaining accurate empirical data.

70   Unlike some of the other input parameters such as porosity, the column height

71   cannot be calculated directly from well logs alone. Instead, three measurements are

72   required: the depth of the hydrocarbon-water contact (fluid contact), the structural

73   apex and the spill point (Fig. 2). The fluid contact can be estimated using well logs

74   and pressure data, however, calculation of the apex and spill point depths requires a

75   reliable top reservoir depth map, since the majority of exploration wells tend to be

76   drilled in down-flank positions. In turn, this requires access to 3D seismic data and a

77   velocity model for depth conversion. This data- and time-intensive approach may

78   explain why few studies of this kind have been carried out before.

79   A number of previous empirical reviews have measured hydrocarbon columns in

80   areas such as the Norwegian Continental Shelf (NCS), Malay Basin and Gulf of

81   Mexico, and all conclude that the observed column heights follow a lognormal

82   distribution (Fosvold et al., 2000; Niemann, 2000; Tanjung, 2014). This result is

83   largely representative of the type of distribution (Fig. 3A) that is widely used in oil and

84   gas exploration as a default for pre-drill volume estimation, regardless of the size of

85   the trap height or burial depth of the prospect. Two other types of commonly used

86   distributions are the normal distribution (Fig. 3B) and uniform distribution (Fig. 3C).

87   Deciding which distribution best describes the column height uncertainty has a

88   significant impact on the pre-drill volume range of a hydrocarbon prospect, and will

89   often determine whether an exploration well is drilled or not.

90   Using the geometry of a prospect to determine the pre-drill column height distribution

91   has only been incorporated into a handful of published studies. Graham et al. (2015)

92   concluded that integration of the trap height, genetic history and geological setting of

93   the prospect is likely to result in the most appropriate column height distribution.

94   Additional contributions by Schlömer and Krooss (1997) state the influence of area-

95   to-relief ratio on the potential discoverable hydrocarbon column. There is scope

96   therefore to introduce a new approach that directly links the pre-drill column height

4

97 distribution to the prospect's geometry, specifically the trap height and burial depth /

98 overburden thickness.

99 This piece of work is primarily concerned with presentation of the empirical data

100 collected across the NCS, as well as identifying trends and correlation between

101 subsets of the data. The 242 measured discoveries are located in a number of basins

102 spanning the Barents Sea, Norwegian Sea and Northern North Sea, and as such,

103 mix a range of different structural and stratigraphic settings. To explore the possible

104 underlying causes of the identified trends presented herein, the data would have to

105 be sub-divided allowing like-for-like basins to be compared. Subsequent technical

106 assessment of subsurface data covering each of the basins would require additional

107 time and methods, a process that demands its own study. It should also be noted that

108 the 242 data points analyzed for this study correspond to discovery cases only. This

109 study is primarily concerned with reducing the uncertainty in prediction of

110 hydrocarbon columns in success-case scenarios, therefore dry wells and causes of

111 failure fall outside the scope of work.

112 This study has three main aims. Firstly, to collect and present a large empirical

113 dataset of measured hydrocarbon column heights, associated trap heights, burial

114 depths, and trap-fill ratios for 242 discoveries across the NCS. Secondly, to identify

115 trends between the measured variables, and to analyze the role of trap-height and

116 burial depth on observed hydrocarbon column heights. Thirdly, to use the results of

117 such analysis to challenge common assumptions regarding column height probability

118 distributions.

119 **2. Study area and methodology**

120   The oil and gas discoveries used in this study are distributed across the NCS in three

121   different regions: the Barents Sea, the Norwegian Sea and the Northern North Sea

122   above 61°N (Fig. 4). Of the 242 discoveries, 123 are located in the Norwegian Sea,

123   81 in the Northern North Sea and 38 in the Barents Sea. The fields and associated

124   structural elements that have been measured as part of the study are summarized in

125   Table 2.

126   The NCS was selected for several reasons. Firstly, it is a good area to study the

127   relationship between trap geometry and hydrocarbon column heights because the

128   majority of the basins in the study areas have received plentiful hydrocarbon charge,

129   so charge limitation is not a significant issue (Doré and Jensen, 1996; Ostanin et al.,

130   2012; Hermanrud et al., 2014). For this reason, it is assumed that the observed

131   variations in column heights and trap-fill ratios are primarily a result of seal behaviour

132   and not because of a lack of charge (Hermanrud and Bols, 2002; Bolås and

133   Hermanrud, 2003; Halland et al., 2013). Secondly, the Norwegian Petroleum

134   Directorate (NPD) provides a large repository of well data, of which many details

135   become public two years after drilling and fully public after 20 years. Access to such

136   well-organized data is particularly helpful when ascertaining the fluid contact depth,

137   which can be directly taken from descriptions in the well reports or from pressure

138   data. Thirdly, the publically available seismic data covering the three regions has

139   been widely interpreted and a large number of good quality, top reservoir maps were

140   made available for this study. Maps were taken either from previous prospect

141   analyses or from regional maps, which were subsequently reinterpreted in more

142   detail where required.

143   Since the vast majority of the available seismic datasets are in the time domain, a

144   regional velocity cube was used to depth convert the top reservoir time (TWT) maps

145 into depth. Top reservoir depth maps were crosschecked against well tops to assess

146 if any depth shift was required. Access to such maps and well data ensures that the

147 relevant data required to calculate the column height, trap height and burial depth is

148 widely available across most of the NCS. However, the assimilation and quality

149 control of the data, which is necessary to measure the apex and spill point depths, is

150 more time consuming. Figure 5 shows an example of such data collection for

151 discovery wellbore 7121/7-1, which is part of the Snøhvit field in the southwestern

152 Barents Sea (Linjordet and Olsen, 1992). The top reservoir surface was mapped in

153 two-way-time, depth-converted and checked against the depth of the top reservoir in

154 the well. The fluid contact was taken from the publically available NPD fact pages

155 and crosschecked against observations and pressure measurements contained

156 within the final well report. The trap-fill ratio was then calculated based on what

157 proportion of the trap height was occupied by the hydrocarbon column (trap-fill ratio =

158 hydrocarbon column height / trap height).

159 As with all subsurface interpretation, and in particular depth conversion, we

160 acknowledge that there will be inaccuracies associated with the apex and spill point

161 depths for individual discoveries (Etris et al., 2001; Pon and Lines, 2005). However,

162 such inaccuracies are minimized in this study through local reinterpretation of

163 regional surfaces to increase topographic detail over the structures, as well as tying

164 the depth surfaces to the relevant well-tops after depth conversion. Consequently,

165 confidence in the collection methods and resulting dataset is good.

166 **3. Results**

167 The empirical data collected in this study is presented in a series of graphs that show

168 the range and distribution of measured variables, which includes the trap height,

169 burial depth, column height and trap-fill ratio for each discovery. Cross plots are

170 useful to identify potential correlations between particular variables and therefore

171 demonstrate possible controls on the observed hydrocarbon column heights. In

172 addition, trap-fill ratios calculated for each measured discovery are displayed as

173 proportionally sized data points on regional geological maps.

3.1 Cross plots

175 Figure 6A is a cross plot of hydrocarbon column height and trap height for all 242

176 data points with bordering histograms showing the distribution of data for each

177 variable. The density of data points decreases and becomes more sparsely

178 distributed as the trap height begins to exceed 400m and when column heights begin

179 to exceed 300m, which is shown by a broadening of the 95% confidence interval of

180 the regression line, indicated by the shading. The R-value (the correlation coefficient

181 between the two-plotted variables) of 0.86 indicates that there is a strong positive

182 correlation between trap height and hydrocarbon column height. The linear dashed

183 line on Figure 6A represents the one-to-one relationship between trap height and

184 column height. All points that fall on this line have a trap-fill of 100%, and the

185 structures are considered to be "filled-to-spill". Figure 6B is a cross plot of the

186 hydrocarbon column height and burial depth / overburden thickness. Burial depth

187 values are distributed centrally with the density of data points decreasing towards

188 very low and very high values. The number of hydrocarbon columns recorded in

189 structures with burial depths exceeding 4000m is limited, which is shown by the

190 broadening of the 95% confidence interval either side of the regression line. The R-

191 value of 0.31 shows there is a moderate positive correlation between burial depth

192 and hydrocarbon column height.

193 Figure 7 displays three trap height versus hydrocarbon column height cross plots

194 (Figs. 7A-C) and three burial depth versus hydrocarbon column height cross plots

(Figs. 7D-F) for each of the three regions covered by this study. All three regions

show a strong positive correlation between hydrocarbon column height and trap

height with the corresponding R-values varying between 0.76 (Barents Sea) and 0.88

(Norwegian Sea). Note the difference in measured trap heights across the three

regions. In the Northern North Sea and Norwegian Sea they reach up to 700m,

whereas the maximum trap height observed in the Barents Sea is just over 400m.

Figures 7D-F show a weak to moderate positive correlation between burial depth and

column height. The Northern North Sea has the lowest R-value of 0.16 and the

Barents Sea has the highest at 0.47. Again, note the difference in the range of burial

depths across the three regions. Hydrocarbon columns measured in the Northern

North Sea and Norwegian Sea are buried between 1000 and 5000m. However, in the

Barents Sea the discoveries are buried at shallower depths, between 200 and

3000m. The maximum hydrocarbon column observed in the Northern North Sea is

452m (well 34/8-7), 680m in the Norwegian Sea (Åsgard discovery) and 296m in the

Barents Sea (Iskrystall discovery).

3.2 Spatial distribution of trap-fill

Trap-fill ratio, a measure of how much of the trap height is occupied by the

hydrocarbon column, is represented in three maps in Figure 8. Each colored,

proportionally sized circle represents the trap-fill ratio for each discovery. The Barents

Sea (Fig. 8A) contains a broad range of trap-fill ranges, particularly in the

Hammerfest Basin, which contains discoveries with all ranges of trap-fill. 100% trap-

fill is most prevalent at the basin margins. The other major cluster of discoveries is

located on the Polhem Sub-platform, where the measured structures range from 50

to 100% filled. Figure 8B shows the distribution of observed trap-fill ratios in the

Norwegian Sea. There is a dense clustering of data points along the axis of the

220   Revfallet Fault Complex, which borders the Halten and Donna Terrace. The majority

221   of the discoveries have a trap-fill ratio of 75% or more, with a few interspersed

222   discoveries with lower levels of trap-fill. The cluster of points on the Nyk High, close

223   to the Aasta Hansteen field, shows that most discoveries in this area tend to be 100%

224   filled. Figure 8C shows the trap-fill distribution across the Northern North Sea. Similar

225   to the Norwegian Sea, the majority of discoveries are filled-to-spill, however, they are

226   more widely distributed and tend to be located more closely to discoveries with lower

227   trap-fill ratios of between 50 and 75%, for example on the Lomre Terrace and

228   Tampen Spur.

229   **4. Data analysis**

230   The empirical dataset was evaluated using a forward probability model, otherwise

231   known as a forward probability-tree, which required each input variable (trap height

232   and burial depth) and output variable (trap-fill ratio) to be categorized into a series of

233   discrete bins. A 3x3 probability distribution matrix is then populated by the forward

234   probabilities calculated in the probability tree to assess how the trap fill ratio varies

235   with trap height and burial depth. A more detailed explanation of this workflow is

236   described below.

237   *4.1 Forward probability model*

238   A forward probability or 'decision tree' approach is a useful tool to assess what

239   influence (if any) the trap height and burial depth have on the trap-fill ratio, and to see

240   if the relationship between them can be used in a predictive manner. The method

241   was chosen to display the distribution of trap-fill ratios for different ranges of trap

242   height and burial depth. The number of bins that define the output variable, in this

243   case, the trap-fill ratio, defines the first set of branches in the forward probability tree

244   (Fig. 9). The number of bins associated with each input variable, i.e. the trap height

245   and burial depth, determine the number of branches that define the second and third

246   decision levels. The total number of branches is equal to the product of the number of

247   bins for each input and output variable, multiplied together. Once the tree has been

248   populated, the probability for each calculated outcome is normalized against other

249   outcomes that share similar trap height and burial depth values. This normalization

250   step is necessary to calculate the probability of finding a given trap-fill ratio for each

251   combination of trap height and burial depth values.

252   *4.2 Binning the data*

253   A number of methods can be used to calculate a suitable number of bins for a given

254   dataset (Miller, 1989; Wand, 1997). One of the simplest approaches is to set the

255   number of bins equal to the square root of the total number of values in the dataset,

256   otherwise known as the square-root choice method. This gives approximately 15 bins

257   of equal width for each variable, as illustrated in Figures 10A-C. However, using 15

258   bins for each of the three variables in a probability tree would result in 3375

259   probabilities (15x15x15), which far exceeds the actual size of the dataset (242). For

260   the purpose of this study, it is necessary to cap the number of bins to avoid such a

261   large number of probabilities. Each variable is therefore divided into just five bins of

262   equal width as shown in Figures 10D-F. This has the desired result of reducing the

263   number of possible outcomes to 125 (5x5x5). However, because of the irregular

264   distribution of values across each variable, some bins contain very few or no values

265   at all. This becomes problematic when calculating probabilities for certain

266   combinations of trap-fill, burial depth and trap height, with too many zero probabilities

267   being returned. To avoid this issue, bins of variable width must be used in order to

268 allow the number of values to be more evenly redistributed across each bin (Figs

269 10G-I) (Miller, 1989).

270 Burial depth was divided into three bins: 0-1500m, 1501-3000m and >3000m (Fig

271 10G), and the trap height was also divided into three bins: 0-150m, 151-300m and

272 >300m (Fig. 10H). The trap-fill ratio was divided into four bins corresponding to 0-

273 50%, 51-75%, 75-99% and 100% trap-fill (Fig. 10I). 100% trap fill is assigned its own

274 bin since nearly half of the measured discoveries (111/242) recorded this level of

275 trap-fill (Fig. 9). Relatively few discoveries had trap-fill values of 50% or lower

276 (31/242), so this category was not further subdivided. The total number of bins gives

277 a workable number of 36 possible outcomes (4x3x3), with only two out of the 36

278 outcomes having a zero probability. These two zero probability outcomes are both

279 caused by a lack of discoveries where the trap-fill exceeds 75% in structures with

280 trap heights above 300m and burial depths of less than 1500m (Fig. 9).

281 *4.3 Probability distribution matrix*

282 The 3x3-output matrix (Fig. 11) shows how the normalized trap-fill probabilities,

283 calculated in the forward-probability tree, vary across different trap height and burial

284 depth ranges. The observed distribution of trap-fill probabilities does not follow the

285 same pattern for each burial depth and trap height combination and as such, there is

286 not one type of distribution that describes all nine input scenarios. The bullet points

287 below describe the other key observations:

288 • When the trap height is 150m or less (at all burial depths), the probability of 0-99%

289 trap-fill is consistently low, whereas the probability of 100% trap-fill is very high.

290 Furthermore, the probability of recording 100% trap-fill is approximately twice as

291 likely as recording a trap-fill ratio between 0 and 99%.

292   •   For trap heights between 151 and 300m, the distribution of trap-fill ratio is less

293   consistent at different burial depths. When the burial depth is 1500m or less, the

294   most likely trap-fill range is between 51 and 75% and the least likely trap-fill is

295   100%. However, when the burial depth exceeds 1500m, this pattern is reversed

296   and 100% trap-fill becomes the most likely outcome, whilst 0-50% trap-fill

297   becomes the least likely.

298   •   For trap heights exceeding 300m with a burial depth of less than 1500m, 0-50%

299   trap-fill is most likely and there are no discoveries with a trap-fill ratio above 75%.

300   Discoveries with trap heights exceeding 300m at depths of 1501-3000m are most

301   likely to have a trap-fill ratio of 51-75% and least likely to have 100% trap-fill.

302   However, when the burial depth exceeds 3000m, 100% becomes the most likely

303   trap-fill ratio and 0-50% the least likely.

304 To summarize, two main trends are observed. Firstly, as the trap height increases for

305 a given burial depth, the probability of 100% trap-fill progressively decreases and the

306 probability of 0-50% trap-fill progressively increases. Secondly, as the burial depth

307 increases for a given trap height, the probability of 100% trap-fill increases, whilst the

308 probability of 0-50% trap-fill decreases. These reversals in trap-fill ratio distributions

309 are evident across all trap height categories for a given burial depth and for all burial

310 depths for a given trap height.

311 **5. Discussion**

312 *5.1 Determining pre-drill hydrocarbon column height distributions*

313 Across all three regions of the NCS, there is a strong positive correlation between the

314 hydrocarbon column height and trap height. Although it may seem obvious, it is

315 important to recognize that trap height exerts a significant control on the hydrocarbon

316 column when estimating pre-drill column heights. Geometrically, a high-relief

317 structure is more likely to be able to hold a taller hydrocarbon column than a low-

318 relief structure. However, a high-relief structure at shallow depths is significantly less

319 likely to be filled-to-spill than those at greater depths (Fig. 11). A weaker positive

320 correlation exists between the column height and burial depth suggesting that the

321 burial depth exerts some control on column heights, but that the relationship between

322 these variables is more complicated. The correlation between column height and

323 burial depth appears to be strongest in shallower discoveries, as shown by the

324 relatively high correlation coefficient for the Barents Sea (Fig. 7).

325 The 3x3 matrix (Fig. 11) clearly shows that the observed distribution of trap-fill ratios

326 does not stay constant for all combinations of trap height and burial depth. In order to

327 reflect this in the pre-drill volume estimation, the burial depth and height of a prospect

328 should be taken into consideration when selecting the type of probability distribution

329 to use for the hydrocarbon column height. The observed trap-fill ratios for discoveries

330 in trap heights of 150m or less at all burial depths suggest that a strongly negatively

331 skewed distribution is most appropriate for prospects in low-relief structures. A

332 negatively skewed distribution remains applicable when the trap height increases to

333 between 151 and 300m at burial depths of 1500m or more. However, for intermediate

334 trap heights at depths of less than 1500m and for trap heights exceeding 300m with

335 less than 3000m of burial depth, the probability distribution curve should be positively

336 skewed in order to reflect the higher probability of a lower trap-fill ratio.

337 These observations challenge the widely accepted view that the hydrocarbon column

338 should always follow a log normal distribution (Fosvold et al., 2000; Niemann, 2000;

339 Demirmen, 2007). Integration of this approach with other existing methods for column

340 height prediction (e.g. fault seal analysis and buoyancy pressure calculations) should

341 lead to improved estimation of pre-drill hydrocarbon volumes by reducing the

342 prevalence of under- and over-estimation of the hydrocarbon column height in

343 prospect analysis.

344 *5.2 The benefits of using integrative methods*

345 It has been acknowledged that when exploration and production companies integrate

346 a variety of probabilistic methods into their workflows and include base-rate figures,

347 their competitive position tends to improve (Jonkman et al., 2000; Skarr et al., 2002;

348 Milkov, 2017). Adopting this approach when determining appropriate hydrocarbon

349 column distributions is particularly important since it has been widely acknowledged

350 as being the most significant contributor to uncertainty in pre-drill volume prediction.

351 For this reason, acquisition and assessment of hydrocarbon column data will have

352 the largest impact on reducing the overall uncertainty (Floris and Peersmann, 1998;

353 Demirmen, 2007). However, this approach should not replace the need for detailed

354 prospect and trap specific analysis (Graham et al., 2015). Thorough analysis of the

355 structural and stratigraphic components of a prospect is always recommended for

356 meaningful risking and decisions that are taken during drill or drop, or appraisal

357 assessments. Best practice lies in integrating the probability- and geological-based

358 approaches to create a multi-disciplinary workflow for improved assessment of

359 hydrocarbon column uncertainty, and thus improved pre-drill volume prediction.

360 *5.3 Universal implications*

361 The data used in this study is collected from a range of basins located on the NCS.

362 Nevertheless, we recommend that the trends and lessons learnt in this study be

363 applied to basins and prospects that lie outside the NCS. The hydrocarbon column

364 height distribution will always remain an uncertainty when calculating pre-drill

365 volumes, regardless of where the prospect is located. This approach also has the

366 wider benefit of improving the efficiency of the exploration and production of

367 hydrocarbons, which will ultimately help to drive down costs. Improved placement of

368 wildcat, appraisal and development wells will lead to a reduction in the number of

369 redundant wells, helping to reduce emissions that are emitted during the drilling

370 process. This in turn will reduce the negative impact of drilling on the environment,

371 which is timely given the oil and gas industry is increasingly seeking ways to improve

372 its environmental image.

373 *5.4 Future work*

374 This study strongly suggests that burial depth and trap height is used to guide trap-fill

375 and hydrocarbon column height prediction. However, the observed patterns could be

376 strengthened or challenged when more values are added to the dataset. A lack of

377 values, for example in discoveries with trap heights above 300m in burial depths of

378 less than 1500m, may weaken the strength of the observed pattern, but may also be

379 indicative of the type of trap geometries that are encountered at different depths in

380 the subsurface. The same approach should be extended further south on the NCS

381 and into the UK Continental Shelf (UKCS). Where possible, it is recommended that

382 additional data are collected further afield, for example from the Gulf Coast, to

383 investigate if different basins settings influence trap fill distributions across variable

384 trap heights and burial depths. Addition of more data points to the dataset will

385 increase the statistical significance of the results and further improve its power as a

386 tool for guiding pre-drill column height predictions.

387 **6. Summary and conclusions**

388 This study presents an empirical dataset across the NCS that includes

389 measurements of the trap height, burial depth, hydrocarbon column and trap-fill ratio

390 of 242 fields and discoveries. To the best of the authors' knowledge, this is the first

391 study of its kind. The key findings from this work are summarized below:

392 • Simple statistical analysis of the dataset reveals a strong correlation between

393 trap height and hydrocarbon column height, and a weaker correlation between

394 burial depth and hydrocarbon column height.

395 • A forward probability approach was used to calculate the probability of a given

396 trap-fill ratio for different combinations of trap height and burial depth ranges. The

397 results are visualized in a 3x3 matrix, which can be used to demonstrate the

398 distribution of trap-fill ratios in discoveries with similar trap heights and burial

399 depths.

400 • The distribution of trap-fill ratios does not stay constant across all trap height and

401 burial depth ranges. When the trap height starts to increase, for a given burial

402 depth, the probability of 100% trap-fill diminishes and the probability 0-50% trap-

403 fill increases. Similarly, as the burial depth increases for any given trap height,

404 the probability of 100% trap-fill increases whilst the probability of 0-50% trap-fill

405 decreases.

406 • Pre-drill column height prediction should be adjusted according to the geometry

407 and burial depth of the prospect, rather than applying a fixed statistical

408 distribution to all prospects. Integration of this empirical approach with

409 consideration of trap-specific details can make a significant contribution to

410 improving the predictability of hydrocarbon column heights in undrilled prospects.

411 This, in turn, will help to reduce the overall uncertainty associated with pre-drill

412 volume estimation in exploration.

413   • This method of data collection and analysis should be repeated for more

414   discoveries across the NCS and the neighboring UKCS. Inclusion of data from

415   different hydrocarbon provinces, such as the Gulf Coast would also help to

416   increase the size and geographical spread of the dataset. This leads to more

417   meaningful statistical outcomes and enhances the predictive power of the

418   dataset.

419   • Estimation of the hydrocarbon column remains a constant uncertainty when

420   assessing pre-drill volumes for all prospects, regardless of location. It is therefore

421   recommended that data collections methods and lessons learnt from this study

422   are applied universally, and integrated into current methods that are used to

423   estimate pre-drill hydrocarbon column heights for prospects worldwide.

424

References

Bolås, H.M.N. and Hermanrud, C., 2003, Hydrocarbon leakage processes and trap retention capacities offshore Norway: Petroleum Geoscience, v. 9, no. 4, p. 321-332, doi:10.1144/1354-079302-549.

Demirmen, F., 2007, Reserves estimation: the challenge for the industry: Journal of Petroleum Technology, v. 59, no. 5, p. 80-89, doi:10.2118/103434-JPT.

Doré, A.G. and Jensen, L.N., 1996, The impact of late Cenozoic uplift and erosion on hydrocarbon exploration: offshore Norway and some other uplifted basins: Global and Planetary Change, v. 12, no. 1-4, p. 415-436, doi:10.1016/0921-8181(95)00031-3.

Etris, E.L., Crabtree, N.J., Dewar, J. and Pickford, S., 2001, True depth conversion: more than a pretty picture: CSEG recorder, v. 26, no. 9, p. 11-22.

Floris, F.J. and Peersmann, M.R., 1998, Uncertainty estimation in volumetrics for supporting hydrocarbon exploration and production decision-making: Petroleum Geoscience, v. 4, no. 1, p. 33-40, doi:10.1144/petgeo.4.1.33.

Fosvold, L., Thomsen, M., Brown, M., Kullerud, L., Ofstad, K. and Heggland, K., 2000, Volumes before and after exploration drilling: results from the project: Evaluation of Norwegian Wildcat Wells (Article 2): Norwegian Petroleum Society Special Publications, v. 9, p. 33-46, doi:10.1016/S0928-8937(00)80007-7.

Garb, F.A., 1988, Assessing Risk in Estimating Hydrocarbon Reserves and in Evaluating Hydrocarbon-Producing Properties: Journal of Petroleum Technology, v. 40, no. 6, p. 765-778, doi:10.2118/15921-PA.

447   Graham, C.B., Savrda, A.M., Davis, S., Walker, P.E., Sykes, M.A. and Corona, F.V.,

448   2015, Improving Hydrocarbon Column Height Estimates: Results From a Global

449   Synthesis (abs): AAPG Search and Discovery article 90216, accessed August 20th,

450   2019,

451   http://www.searchanddiscovery.com/abstracts/html/2015/90216ace/abstracts/208845

452   0.html

453   Halland, E.K., Mujezinonić, J., Riis, F., 2013, CO2 Storage Atlas, Barents Sea,

454   accessed September 2nd, 2019, https://www.npd.no/en/facts/publications/.

455   Hermanrud, C. and Bols, H.M.N., 2002, Leakage from overpressured hydrocarbon

456   reservoirs at Haltenbanken and in the northern North Sea: Norwegian Petroleum

457   Society Special Publications, v. 11, p. 221-23, doi:10.1016/S0928-8937(02)80017-0.

458   Hermanrud, C., Halkjelsvik, M.E., Kristiansen, K., Bernal, A. and Strömbäck, A.C.,

459   2014, Petroleum column-height controls in the western Hammerfest Basin, Barents

460   Sea: Petroleum Geoscience, v. 20, p. 227-240, doi:10.1144/petgeo2013-041.

461   Jonkman, R. M., Bos, C. F. M., Breunese, J. N., Morgan, D. T. K., Spencer, J. A., and

462   Søndenå, E. 2000, Best Practices and Methods in Hydrocarbon Resource

463   Estimation, Production and Emissions Forecasting, Uncertainty Evaluation and

464   Decision Making; Society of Petroleum Engineers, doi:10.2118/65144-MS

465   Linjordet, A. and Olsen, R.G., 1992, The Jurassic Snøhvit Gas Field, Hammerfest

466   Basin, Offshore Northern Norway: AAPG Special Volume, M54: Giant Oil and Gas

467   Fields of the Decade 1978-1988, Chapter 22, p. 349-370.

468   Milkov, A.V., 2017, Integrate instead of ignoring: Base rate neglect as a common

469   fallacy of petroleum explorers: AAPG Bulletin, v. 101, p. 1905-1916, doi:

470   10.1306/032717162817003.

471   Miller, J.C., 1989, Statistics for advanced level: Cambridge University Press., 442 p.

472   Niemann, J.C., 2000, Statistical Distributions of Hydrocarbon Column Heights for Gulf

473   of Mexico Trap Types and Seals (abs): AAPG Discovery series No. 1, last accessed

474   18th September 2019,

475   http://archives.datapages.com/data/specpubs/discovery1/D0127/D0127001.HTM.

476   Norwegian Petroleum Directorate, 2019, Factpages and Factmaps, accessed 30th

477   August 2019, https://factmaps.npd.no/arcgis/rest/services/FactMaps/3_0/MapServer.

478   Ostanin, I., Anka, Z., di Primio, R. and Bernal, A., 2012, Identification of a large

479   Upper Cretaceous polygonal fault network in the Hammerfest basin: Implications on

480   the reactivation of regional faulting and gas leakage dynamics, SW Barents

481   Sea: Marine Geology, v. 332, p. 109-125, doi:10.1016/j.margeo.2012.03.005.

482   Pon, S. and R. Lines, L., 2005, Sensitivity analysis of seismic depth migrations:

483   Geophysics, v. 70, p. S39-S42, doi:10.1190/1.1897036.

484   Schlömer, S. and Krooss, B.M., 1997, Experimental characterisation of the

485   hydrocarbon sealing efficiency of cap rocks: Marine and Petroleum Geology, v. 14, p.

486   565-580, doi:10.1016/S0264-8172(97)00022-6.

487   Skaar, K.J., Spencer, A.M., Alexander-Marrack, P. and Støle, G., 2000, Suggestions

488   for an improved exploration process - lessons from the project: Evaluation of

489   Norwegian Wildcat Wells (Article 4): NPF Special Publication no. 9, p. 57-63.

490   Tanjung, B.A., 2014, Statistical Distributions of Hydrocarbon Column Heights for

491   Determining Acreage of Prospect to Estimate Hydrocarbon Resources in Kakap

492   Block (abs), last accessed August 12th 2019,

493   http://archives.datapages.com/data/ipa_pdf/2014/IPA14-G-173.htm

494   Wand, M.P., 1997, Data-Based Choice of Histogram Bin Width: The American

495   Statistician, v. 51, p. 59-64, doi:10.1080/00031305.1997.10473591.

496

497 **Table. 1** A list of defined inputs that are required to calculated hydrocarbon volumes

498

Input	Definition
Hydrocarbon column height	The height of a continuous hydrocarbon column measured from the apex of the structure down to the hydrocarbon-water contact
Recovery factor	The percentage of hydrocarbons that can be produced from the volume of hydrocarbons initially in place
Net/gross ratio	The reservoir rock thickness that has sufficient porosity/permeability from which hydrocarbons can be produced divided by the total reservoir thickness (see below for definition)
Gas fraction of column height	Proportion of the hydrocarbon column height occupied by gas
Porosity (effective)	Interconnected space within the rock that can be occupied by moveable fluids. Excludes isolated pore spaces.
Reservoir thickness	Thickness of the stratigraphic unit that contains the reservoir beds
Oil saturation	Fraction of the pore space occupied by oil
Area	Areal extent of the reservoir contained within the closure at the depth of the fluid contact
Formation volume factor (oil)	The oil volume at reservoir conditions divided by the oil volume at standard conditions (surface conditions)
Depth-dependent area	Function that describes the relationship between depth and the areal extent of the reservoir contained within the closure

499 **Table 2.** A list of structural elements, and fields and discoveries that have been

500 measured in this study

Region	Structural elements	Fields and Discoveries
Barents Sea	Hammerfest Basin, Loppa High, Måsøy Fault Complex, Nysleppen Fault Complex, Polhem Sub-Platform, Troms-Finmark Fault Complex	Alke, Bamse, Goliat, Iskrystall, Johan Castberg, Nucula, Norvarg, Snøhvit, Wisting
Norwegian Sea	Dønna Terrace, Halten Terrace, Nyk High, Rås Basin, Vøring Basin,	Aasta Hansteen, Åsgard, Alve, Bauge, Draugen, Dvalin, Fenja, Heidrun, Hyme, Kristin, Linnorm, Maria, Marulk, Mikkel, Morvin, Njord, Norne, Ormen Lange, Skarv, Skuld, Trestakk, Tyrihans, Urd, Ærfugl
Northern North Sea	Gullfaks Block Zone, Lomre Terrace, Marflo Spur, Måloy Slope, Tampen Spur, Tjalve Terrace, Uer Terrace	Byrding, Fram, Gjøa East, Gjøa, Gullfaks, Gullfaks Sør, Knarr, Kvitebørn, Snorre, Stafjord, Statfjord Nord, Statfjord Øst, Sygna, Tordis, Tordis Borg, Tordis Øst, Vega, Vega South, Valemon, Vigdis, Vigdis Sørøst, Vigdis West, Visund

501

Figure captions

Fig.1. A typical tornado plot generated during pre-drill volume estimation (oil case). It shows the sensitivity of the calculated hydrocarbon reserves to changes in the input variables. Changes in the hydrocarbon column height has the largest effect of all the inputs for the majority of exploration prospects. P10 (possible) means that there is at least a 10% probability that the actual volume of hydrocarbons recovered equals or exceeds the P10 estimate (high estimate). P90 (proved) means that there is at least a 90% probability that the actual volume of hydrocarbons recovered equals or exceeds the P90 estimate (low estimate). Input data are sourced from the NCS.

Fig. 2. A schematic diagram of a fault-bounded hydrocarbon trap. The depth of the structural apex, fluid contact and spill point must be measured in order to calculate the following dimensions: burial depth (a), hydrocarbon column height (b) and trap height (c).

Fig. 3. Three different types of probability distributions. (A) shows a lognormal distribution, which is recognized by a skewed profile that is characterized by an initial steeply dipping limb leading to a peak followed by a longer more gradual dipping limb. (B) shows a normal distribution, which is typically symmetrical about x when x is equal to the mean and (C) shows a uniform distribution, in which all values are equally probable.

Fig. 4. A map of the Norwegian Continental Shelf showing the locations of discovery boreholes used in this study. The distribution of boreholes is separated into three regions: the Barents Sea, the Norwegian Sea and the Northern North Sea (above 61°N). The geological structural base map is from the Norwegian Petroleum Directorate (NPD FactMaps, 2019).

Fig. 5. An example of measurements taken from a structure targeted by exploratory well 7121/7-1, in the Snøhvit field in the southwest Barents Sea. (A) is the map of the top reservoir (Stø Fm.) and indicates the location of cross section A-A' in white, the gas-water contact contour (red) and the spill-point contour (black). (B) shows cross section A-A' with seismic and (C) shows cross section A-A' without seismic. The spill point, gas-water contact and apex depths, which are required to calculate the hydrocarbon column height, trap height, trap-fill ratio and burial depth of the discovery are marked on (B)-(C).

Fig. 6. Cross plots of the empirical data. (A) is a cross plot of the trap height and hydrocarbon column height for all measured discoveries. The linear dashed line represents discoveries that record 100% trap-fill and are referred to as 'filled-to-spill'. All points below this line indicate the structure is underfilled. (B) is a cross plot of the burial depth and hydrocarbon column height. Bordering histograms on the x- and y- axes show the distribution of each variable. Both graphs display a blue regression line bordered by a shaded area. The strength of each correlation coefficient is indicated by the rvalue and the shading indicates the 95% confidence interval of the regression line's location.

Fig. 7. Six cross plots for each of the three regions across the Norwegian Continental Shelf. The hydrocarbon column height is plotted against trap height for the Northern North Sea (A), Norwegian Sea (B) and Barents Sea (C). The hydrocarbon column height is plotted against the burial depth for the Northern North Sea (D), Norwegian Sea (E) and Barents Sea (F). Regression lines plotted on each graph indicate the line of best fit and the accompanying rvalue indicates the strength of the correlation coefficient between the two variables. Shading either side of the regression line represents the 95% confidence interval of the regression line's location.

Fig. 8. Spatial distribution of trap-fill ratios for each measured discovery across the Barents Sea (A), Norwegian Sea (B) and Northern North Sea (C). The larger and darker colored the circle, the higher the trap fill ratio, as shown by the largest dark red circle, which represents 100% trap fill. The base map is a structural map outlining the main geological elements (NPD FactMaps, 2019).

Fig. 9. A decision tree, which is used to estimate the probability of encountering a particular trap-fill ratio, given the trap height and burial depth of the structure is known. The trap-fill ratio is the outcome variable and defines the first decision level. It is divided into four branches and the values associated with each branch is defined by the bin widths in Fig. 10I. The subsequent second and third decision levels are defined by the two input variables: the trap height and burial depth. The trap height defines the second decision level, which is divided into three branches. The values associated with each branch are shown by the bins widths in Fig. 10H. The burial depth defines the third decision level and is divided into three branches. The values for each branch are defined by the bins widths in Fig. 10G. The decision tree contains 36 different probable outcomes. Each outcome carries an absolute probability and a normalized probability. The absolute probability is the product of three probabilities, each one associated with one branch at decision level one, two and three. The normalized probability is the absolute probability normalized against other absolute probabilities that share the same trap height and burial depth ranges. There are nine different trap height/burial depth combinations in total.

Fig. 10. A series of bar charts showing the distribution of the burial depths (dark blue), trap heights (medium blue) and trap-fill ratios (light blue) for all measured discoveries across the NCS. (A), (B) and (C) splits each dataset into 15 equally spaced bins. (D) (E) and (F) divides each dataset in into five equally spaced bins. (G)
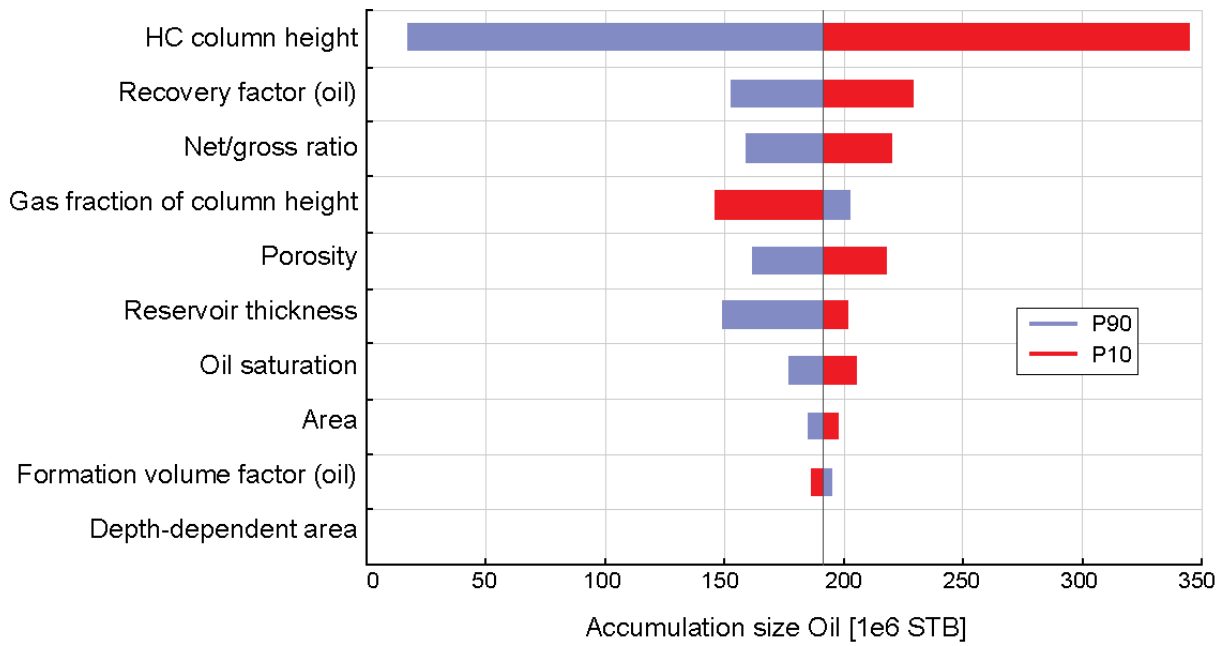
576   divides the burial depth dataset into three bins of unequal width. (H) divides the trap

577   height dataset into three bins of unequal width and (I) divides the trap fill ratio dataset

578   into four bins of unequal width. The bins widths chosen in (G), (H) and (I) determine

579   the number of branches in the decision tree shown in Fig. 9.

580   **Fig. 11**. A three by three probability distribution matrix showing how the probability of

581   different trap fill ratios changes when the trap height and burial depth dimensions

582   vary. Each sub-chart represents the distribution of trap-fill ratio probabilities for each

583   of the nine burial depth (y-axis) and trap height (x-axis) combinations. The nine sub-

584   charts are populated using the normalized probabilities calculated in Fig. 9. The

585   number of measured discoveries in the dataset that corresponds to one of the nine

586   trap height/burial depth combinations is indicated by n.
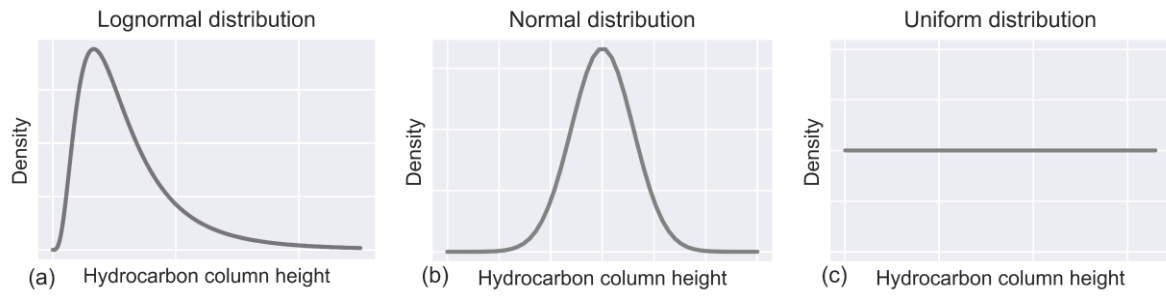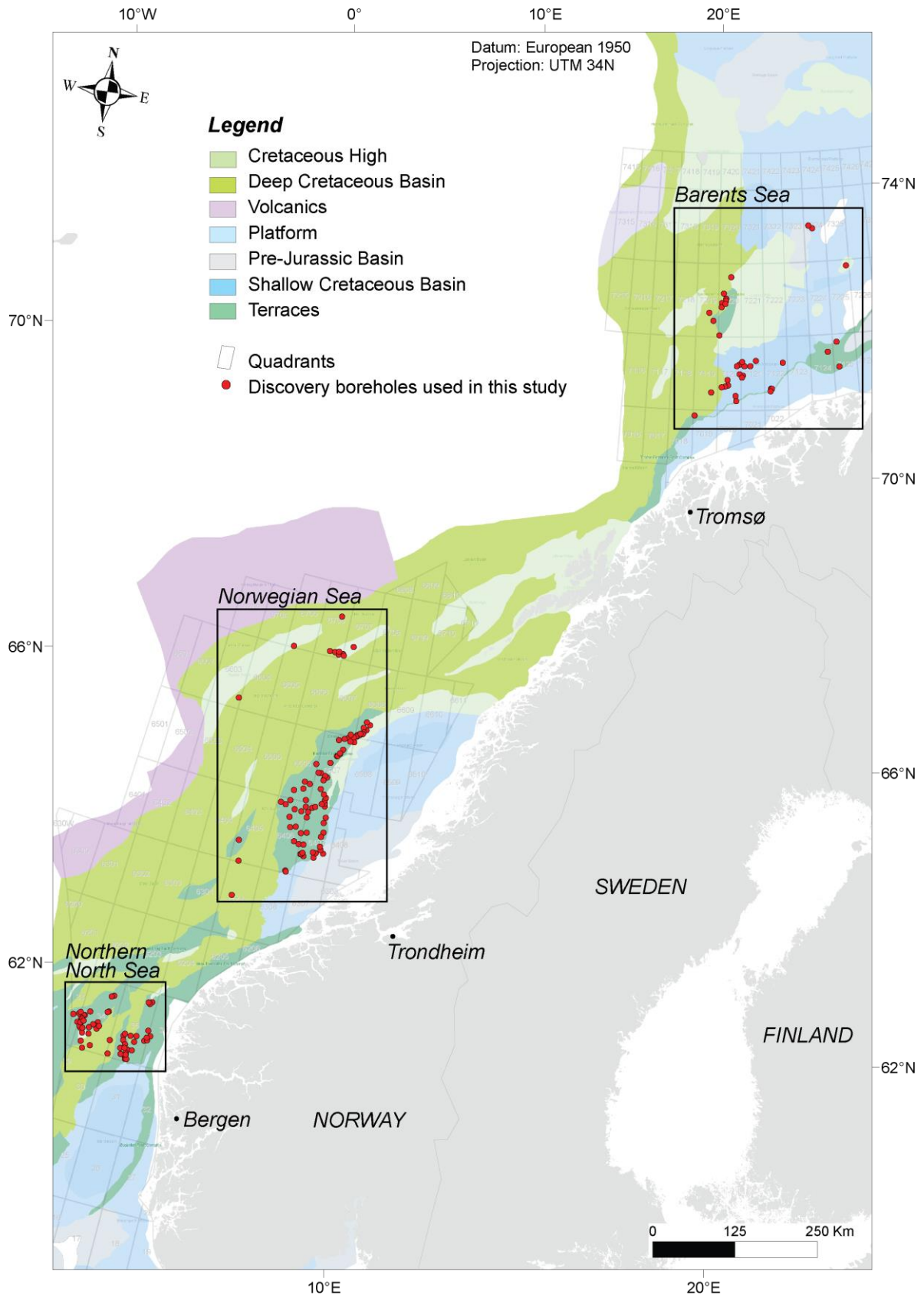
587

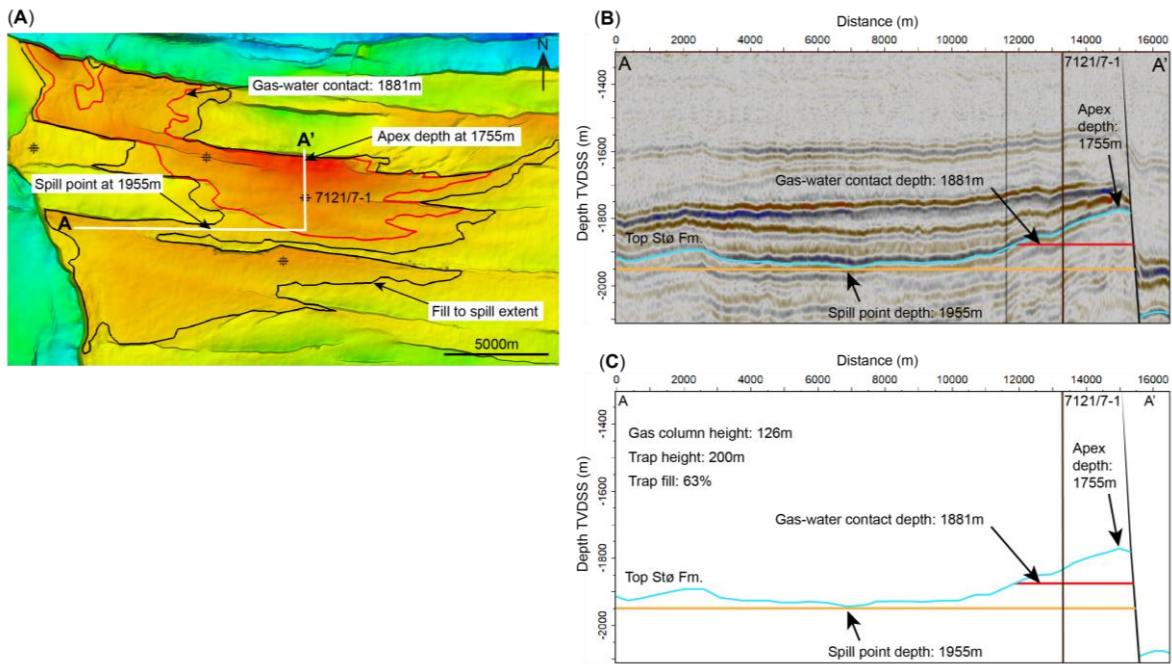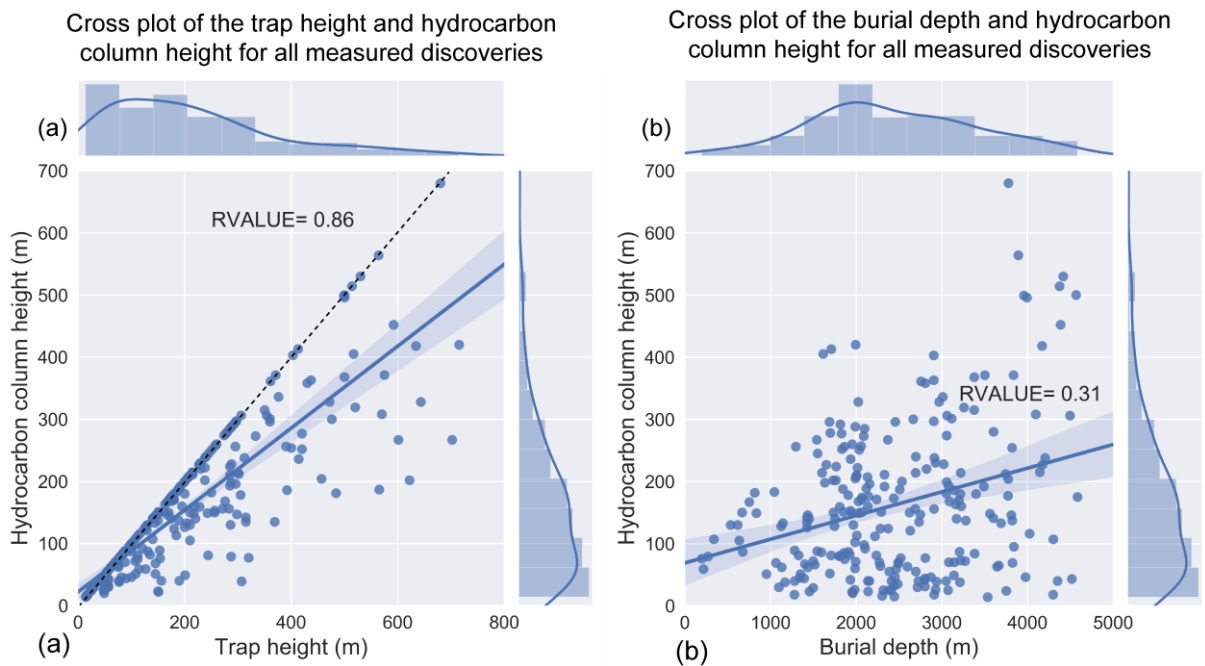588 **Figures**

589 Figure 1

590

591 Figure 2

592

Figure 3

Lognormal distribution

Density

(a) Hydrocarbon column height

Normal distribution

Density

(b) Hydrocarbon column height

Uniform distribution

Density

(c) Hydrocarbon column height
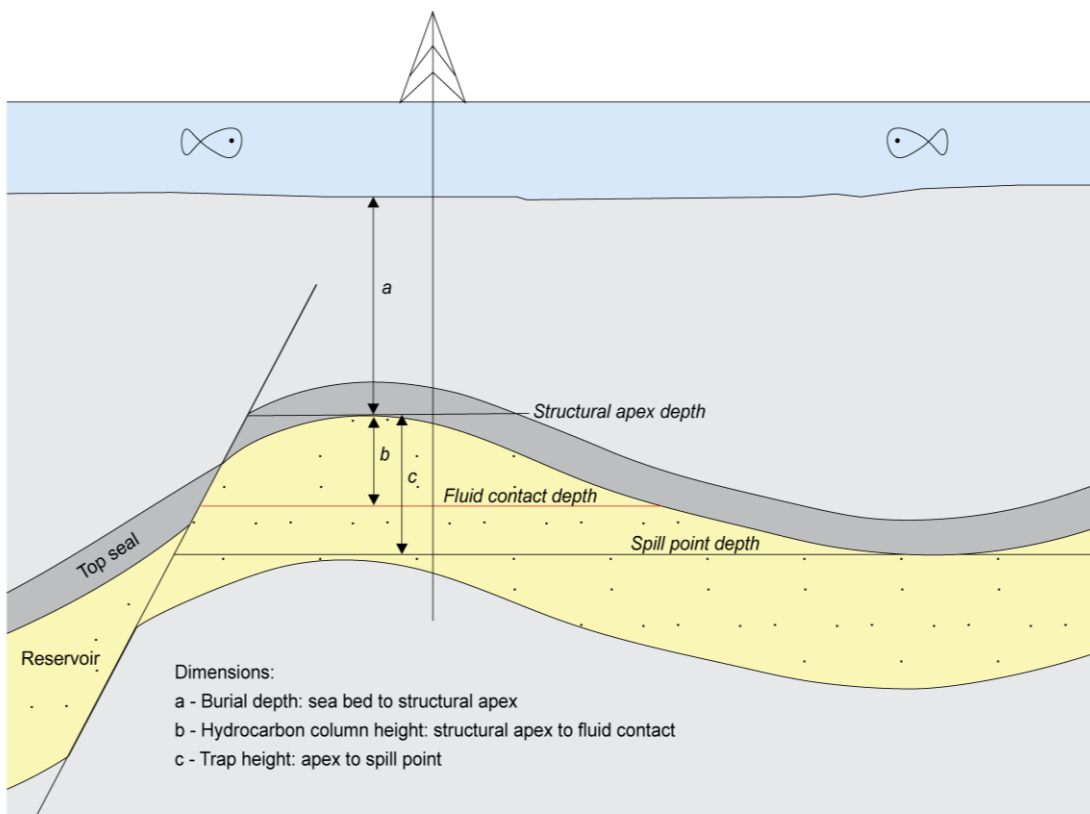
594   Figure 4

596   Figure 5

597

598   Figure 6

Cross plot of the trap height and hydrocarbon column height for all measured discoveries

Cross plot of the burial depth and hydrocarbon column height for all measured discoveries

599

600

601

602   Figure 7
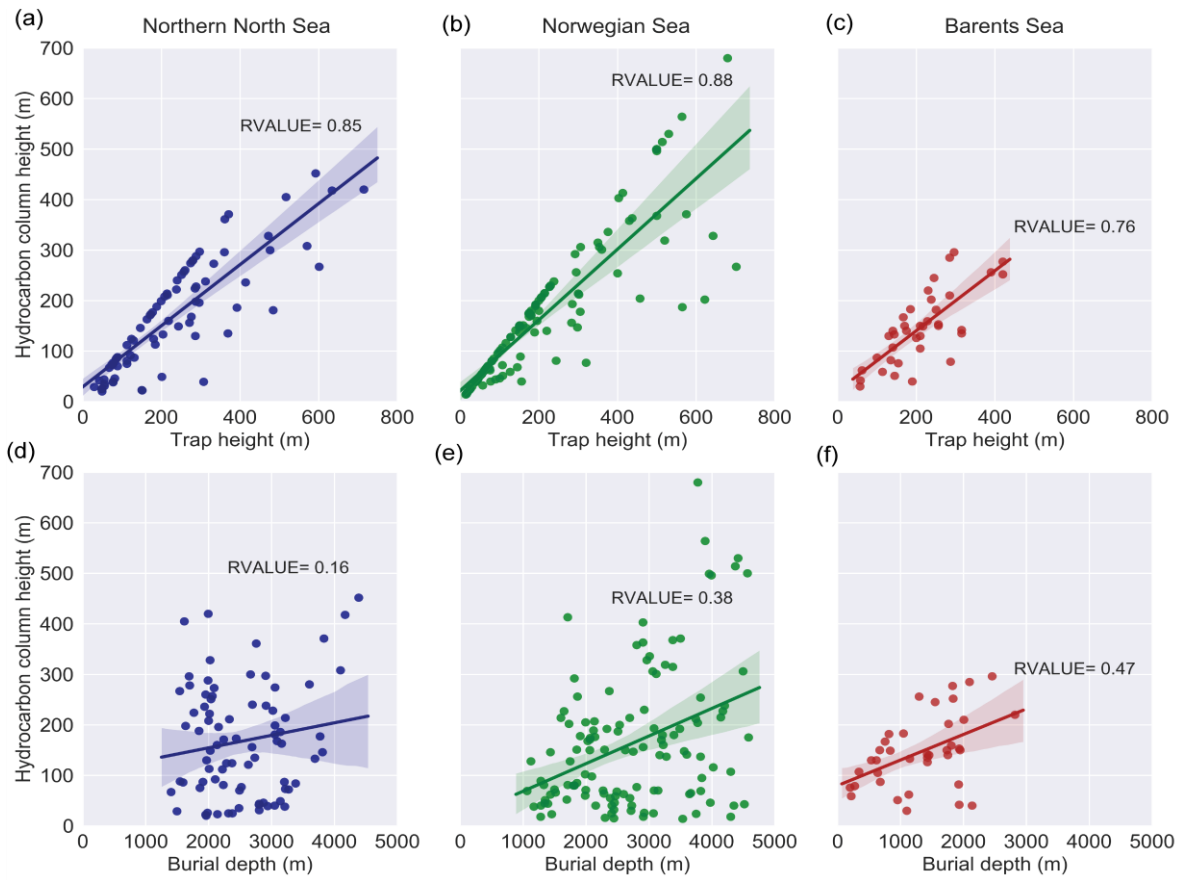
603

604

605

606

607

608

609

610

611

612
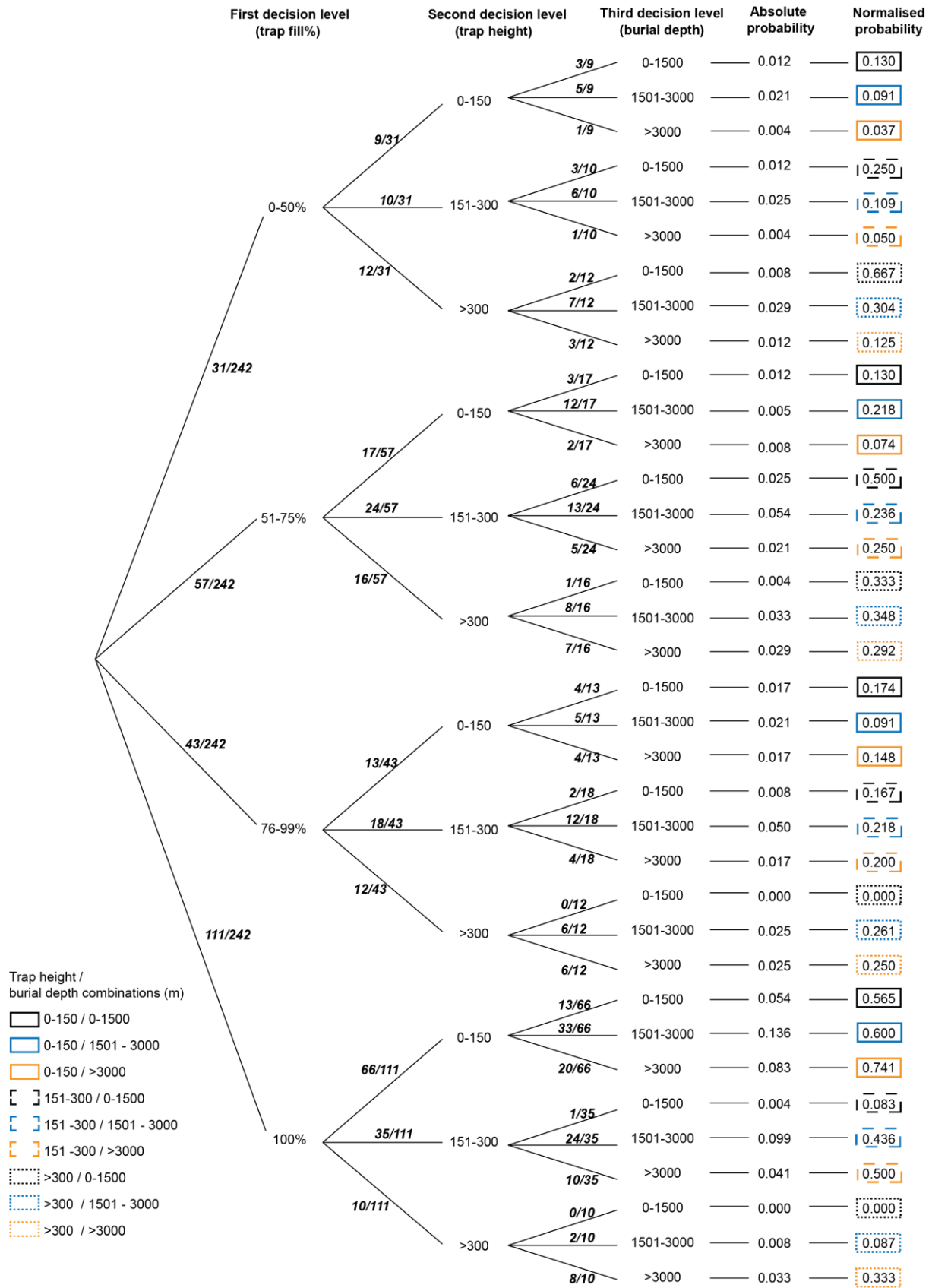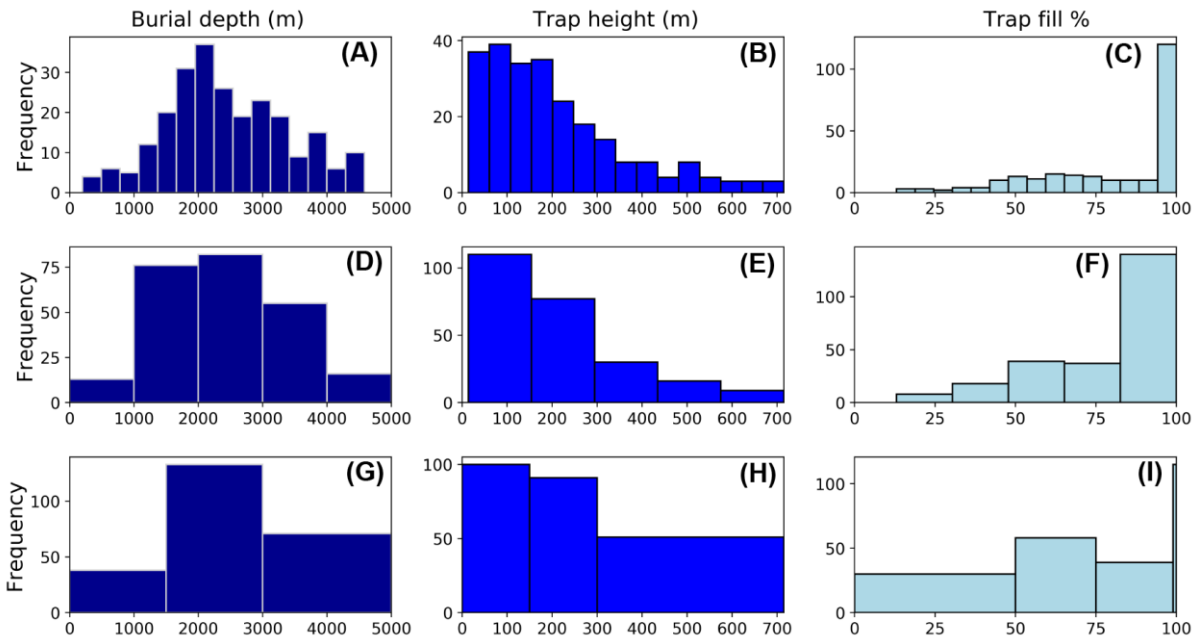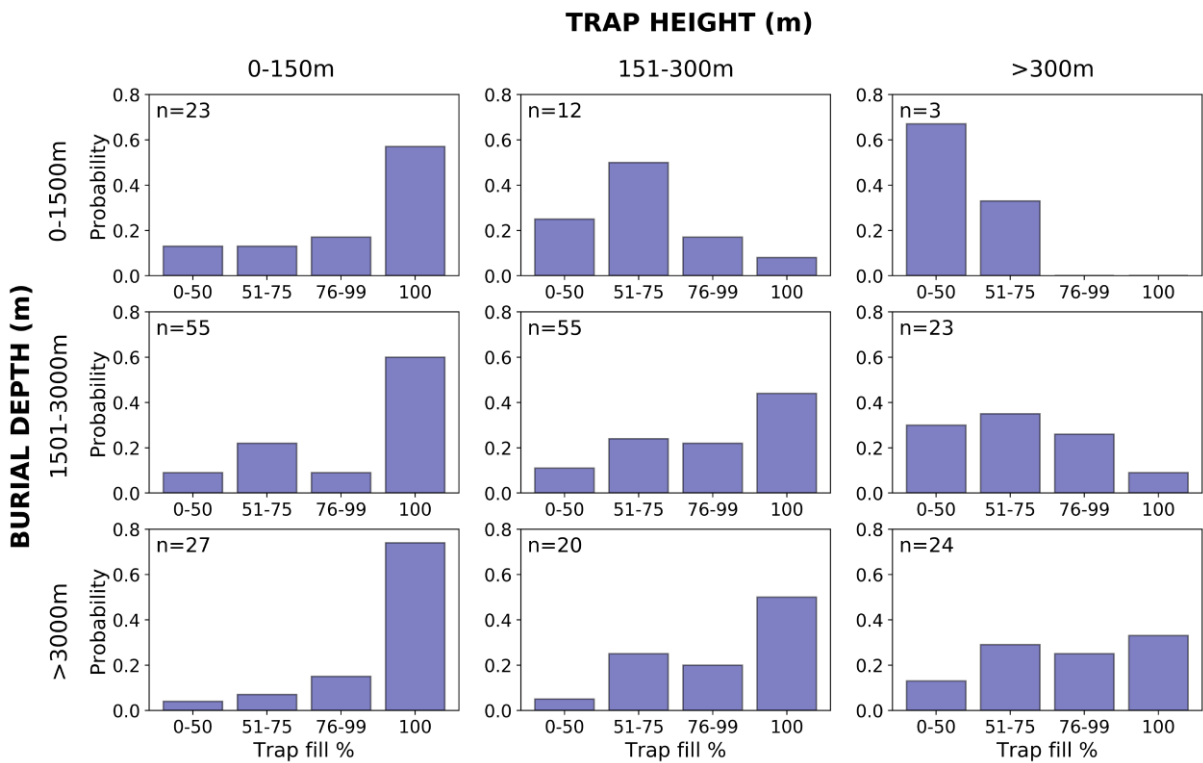
613   Figure 8

614

615   Figure 9

616
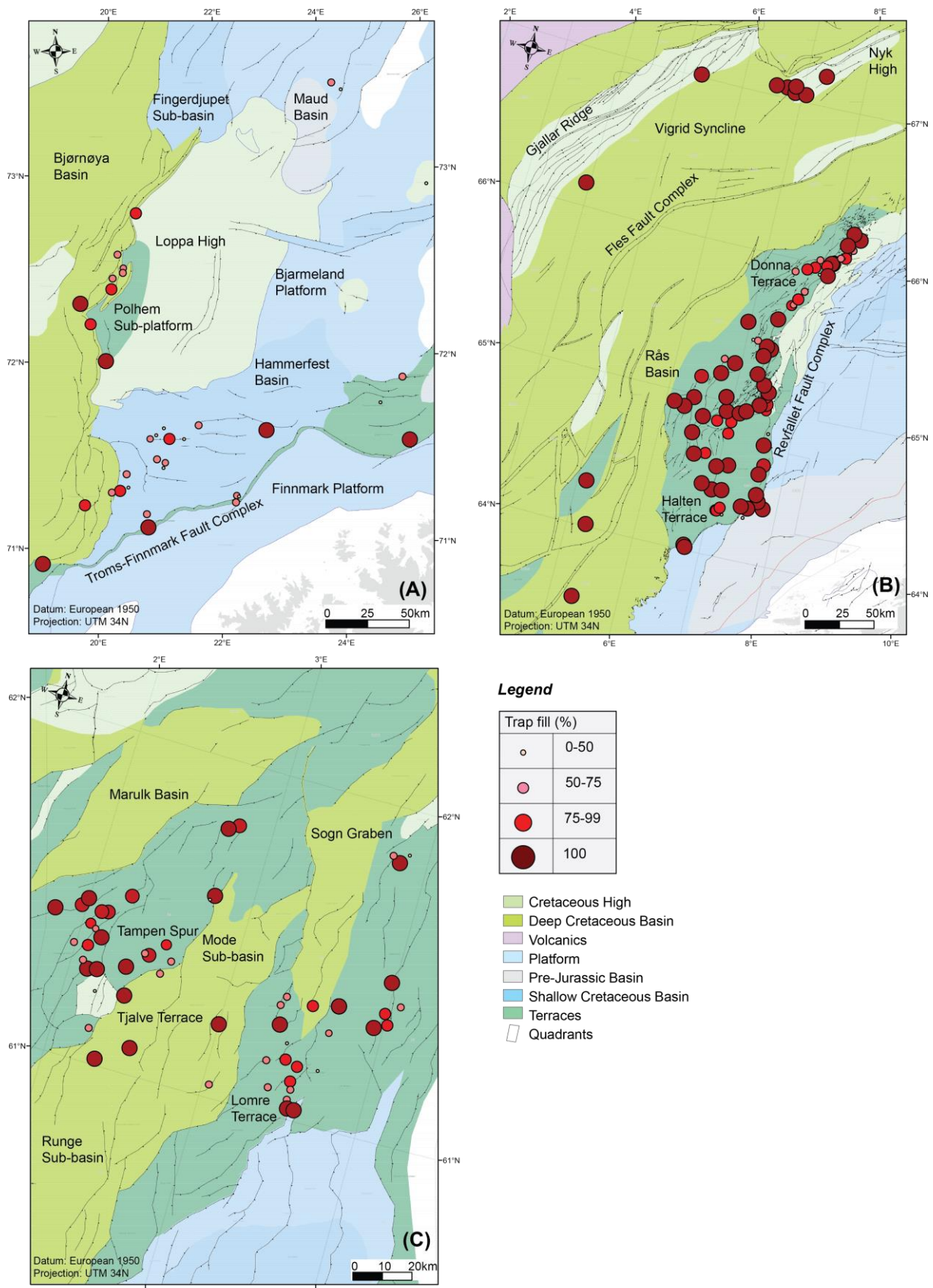
617   Figure 10

618

619   Figure 11

620

621   END